The Redox Behaviour of the Family $(C_{60})[Mo(CO)_2(phen)(dbm)]_n$ ($n = 1-3$) – A Comparison with the Analog $(\eta^2\text{-}C_{70})[Mo(CO)_2(phen)(dbm)]$ (phen = 1,10-Phenanthroline; dbm = Dibutyl Maleate)

Piero Zanello,*[a] Franco Laschi,[a] Arnaldo Cinquantini,[a] Marco Fontani,[a] Kaluo Tang,[b] Xianglin Jin,[b] and Lei Li[b]

Keywords: Fullerenes / Electrochemistry / EPR spectroscopy / Molybdenum / Carbonyl complexes

The electrochemical behaviour of the series $(C_{60})[Mo(CO)_2(phen)(dbm)]_n$ (n = 1–3) has been studied in dichloromethane solution. Each member of the family displays three reversible, fullerene-centred, one-electron reductions at potential values which linearly shift towards more negative potential values by 0.15 V for each appended molybdenum fragment. Such reduction processes are in turn followed by a metal-centred reduction, which causes decomplexation of the C_{60} ligand. EPR spectra recorded on the electrogenerated monoanions $[(C_{60})\{Mo(CO)_2(phen)(dbm)\}_n]^-$ (n = 1, 2) exhibit features indicative of some interaction between the electron entering the fullerene ligand and the metallic centre(s). Comparison with the redox behaviour of the C_{70}-analog $(C_{70})[Mo(CO)_2(phen)(dbm)]$ reveals significant differences; namely that the C_{70}-analog exhibits two reversible one-electron reductions followed by a single two-electron reduction, all of these reductions being centred on the fullerene ligand. A further cathodic step centred on the metallic fragment is present, which, also in this case, causes framework destruction releasing the C_{70} ligand.

Introduction

Metallofullerenes should display a rich redox propensity because the well-known ability of fullerenes to undergo reversibly multiple one-electron transfers[1] is coupled to that of the appended metal fragments. However, only few of them have been studied from the electrochemical viewpoint[2–7] and essentially no data are available for C_{70} complexes.[2] A number of fullerenes containing exohedral multimetallic frames have been structurally characterised. They include binuclear C_{60}-Ir_2,[8,9] -Ru_2,[10] -Si_2,[11] -Fe_2,[2] -Re_2,[3] C_{70}-Ir_2,[12] trinuclear C_{60}-Ru_3,[13] -Os_3,[4] C_{70}-Ru_3,[14] tetranuclear C_{60}-Ir_4,[15] C_{70}-Pt_4,[16] pentanuclear C_{60}-Ru_5,[17] and hexanuclear C_{60}-Pt_6,[18] C_{60}-Ru_6,[17] C_{60}-Ru_5Pt,[17] and C_{70}-Ru_6[14] assemblies. Some of these multimetallic complexes are constituted with a number of identical metal fragments appended to one fullerene ligand, such as $C_{60}[Pt(PR_3)_2]_n$ ($1 \le n \le 4$)[6] and $C_{60}[S_2Fe_2(CO)_6]_n$ ($1 \le n \le 3$).[2] These derivatives have also been studied from the electrochemical viewpoint. Based on these results, we decided to perform a spectroelectrochemical study on the series $(\eta^2\text{-}C_{60})[Mo(CO)_2(phen)(dbm)]_n$ ($1 \le n \le 3$; phen = 1,10-phenanthroline; dbm = dibutyl maleate), Scheme 1.

In addition, we compared the electrochemical behaviour of $(\eta^2\text{-}C_{60})[Mo(CO)_2(phen)(dbm)]$ with that of its C_{70} analog $(\eta^2\text{-}C_{70})[Mo(CO)_2(phen)(dbm)]$. We have already reported on the mononuclear complexes $(\eta^2\text{-}C_{60})[M(CO)_2(phen)(dbm)]$ (M = Mo, W).[7]

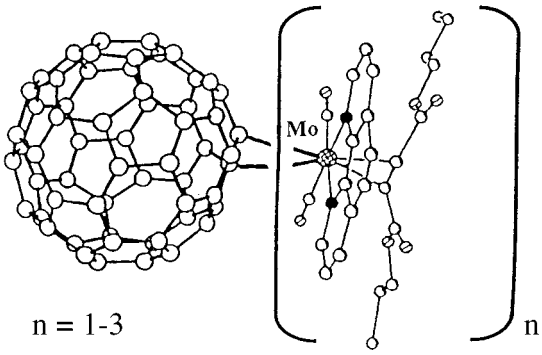

Scheme 1

Results and Discussion

Electrochemistry and Coupled EPR Spectroscopy of $(C_{60})[Mo(CO)_2(phen)(dbm)]_n$

Figure 1 compares the cyclic voltammetric response of the three complexes $(C_{60})[Mo(CO)_2(phen)(dbm)]_n$ (n = 1–3) with that of C_{60}.

A preliminary glance shows that, as with other multimetallic fullerenes,[3,5,6] the di- and (particularly) the tri-molybdenum derivatives contain some amounts of the corresponding mono- and di-metallic precursors. These unwanted precursors do not appear to arise from the electron transfer processes, and further studies will be needed to clarify whether they originate from difficult separation or from dissociation equilibria setting up in solution. An analysis of the responses obtained by varying the scan rate, shows that in the case of $(C_{60})[Mo(CO)_2(phen)(dbm)]$, the first three

[a] Dipartimento di Chimica dell'Università di Siena, Via Aldo Moro, 53100 Siena, Italy
[b] Institute of Physical Chemistry, Peking University, Beijing 100871, P.R.China

  1434–1948/00/0606–1345 $ 17.50+.50/0

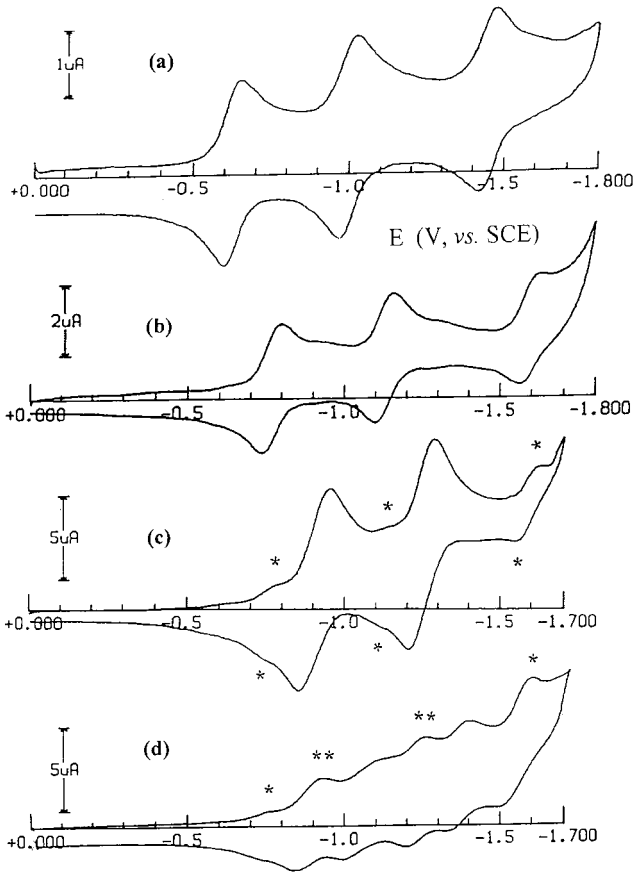

Figure 1. Cyclic voltammetric responses recorded at a platinum electrode in CH_2Cl_2 solutions containing $[NBu_4][PF_6]$ (0.2 mol dm^{-3}) and: (a) C_{60} (saturated solution); (b) $C_{60}[Mo(CO)_2(phen)(dbm)]$ ($6\cdot10^{-4}$ mol dm^{-3}); (c) $C_{60}[Mo(CO)_2(phen)(dbm)]_2$ ($5\cdot10^{-4}$ mol dm^{-3}); (d) $C_{60}[Mo(CO)_2(phen)(dbm)]_3$ ($4\cdot10^{-4}$ mol dm^{-3}); scan rate 0.2 Vs^{-1}; $T = -10$ °C

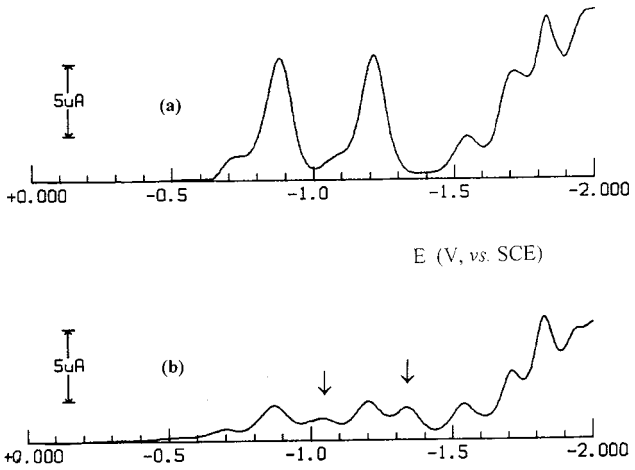

Figure 2. Differential pulse voltammograms recorded at a platinum electrode in CH_2Cl_2 solutions containing $[NBu_4][PF_6]$ (0.2 mol dm^{-3}) and: (a) $C_{60}[Mo(CO)_2(phen)(dbm)]_2$ ($5\cdot10^{-4}$ mol dm^{-3}); (b) $C_{60}[Mo(CO)_2(phen)(dbm)]_3$ ($5\cdot10^{-4}$ mol dm^{-3}); scan rate 0.004 Vs^{-1}; $T = -10$ °C; the arrows point at the processes assumed to be the first and second reduction of the tris-adduct, respectively

reversible one-electron reductions are shifted towards more negative potentials values (by about 0.15 V) with respect to those of free C_{60}, Figure 1b. A fourth reduction, not shown in Figure 1b, is also present at more negative potential values ($E_p \approx -1.9$ V). This reduction involves an ECE mechanism, in which the reduction of the Mo-fragment triggers decomplexation of $[C_{60}]^{3-}$ followed by the concomitant reduction of this trianion to the corresponding tetraanion.[7b] As Figure 1c illustrates, the insertion of the second $Mo(CO)_2(phen)(dbm)$ fragment does not substantially modify the overall reduction sequence, but results in a further cathodic shift of all the redox changes. Based on the relative peak heights of the reduction steps of the monoadduct by-product (monostarred peak-systems in Figure 1c), it seems that the second reduction of the bis-adduct triggers partial decomplexation of one Mo-fragment. Unfortunately, the interpretation of the cyclic voltammetric response of the tris-adduct illustrated in Figure 1d is less straightforward, because of the presence of excessively large amounts of mono- and bis-adducts, the reduction processes of which are labelled by single and double asterisks, respectively. By way of speculation, the reoxidation peak at about −1.0 V seems to be directly associated with the first one-electron reduction of the tris-adduct, the cathodic peak of which is partially overlapped by the second reduction of the monoadduct. Some support to such an assignment could come from the comparison between the differential pulse voltammograms of the bis- and tris- adducts shown in Figure 2, in which the first reduction of the tris-adduct seems to lie at $E_p = -1.04$ V, in between the two reductions of the bis-adduct by-product.

This being allowed, we could tentatively assign the second reversible reduction of the tris-adduct to the peak-system located at about −1.4 V. Because of the complex pattern, any attempt to assign the subsequent steps is ruled out. All the pertinent redox potentials are summarised in Table 1.

Table 1. Formal electrode potentials (V, vs. SCE) for the one-electron reductions exhibited by the metallafullerenes $(C_{60})[MoL]_n$ and $(C_{70})[MoL]$ [L = $(CO)_2(phen)(dbm)$] in dichloromethane, $T = -10$ °C

Complex	$E^{\circ\prime}_{1st}$	$E^{\circ\prime}_{2nd}$	$E^{\circ\prime}_{3rd}$	$E^{\circ\prime}_{4th}$
C_{60}	−0.63	−1.00	−1.45	−1.88
$(C_{60})[MoL]$	−0.77	−1.13	−1.60	−1.86[a]
$(C_{60})[MoL]_2$	−0.91	−1.24	−1.78	−1.92[a]
$(C_{60})[MoL]_3$	−1.04	−1.37	−	−
C_{70}	−0.61	−0.98	−1.41	−1.75
$(C_{70})[MoL]$	−0.71	−1.09	−1.51[b]	−1.82[c]

[a] Peak potential for metal-centred ECE mechanisms; measured at 0.2 Vs^{-1}. – [b] Averaged potential value for an overlapping two-electron process; see text. – [c] Peak potential for an irreversible process; measured at 0.2 Vs^{-1}.

Further support to the above assignments comes from the trend of the formal electrode potentials of the reduction processes with respect to the number of metal fragments, illustrated in Figure 3.

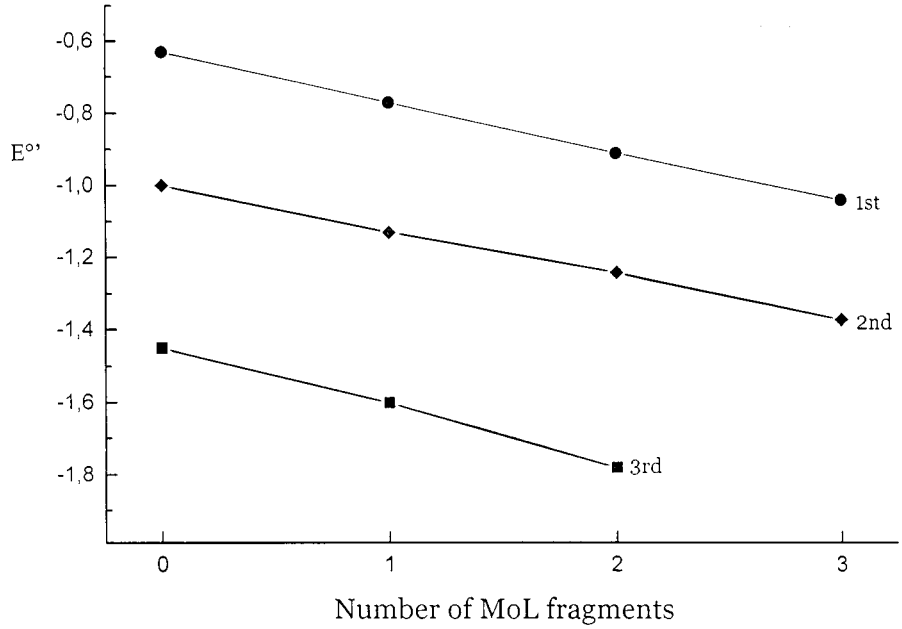

Figure 3. Plot of the formal electrode potentials of the first (1st), second (2nd), and third (3rd) fullerene centred reductions of $C_{60}[Mo(CO)_2(phen)(dbm)]_n$ vs. the number of molybdenum fragments

As it happens, for the series $C_{60}[Pt(PR_3)_2]_n$,[6] the formal electrode potentials of the first reduction increase linearly with the number of metal fragments (correlation coefficient = 1.0); the same trend substantially holds for the subsequent fullerene-centred reductions. This result points out that the electronic effects played by each metal subunit are fully additive. It should however be taken into account that the shifts of the redox potentials must arise either from the inductive effects exerted by the metal fragment(s), which can favour or disfavour the reduction processes, or from the progressive interruption of the double-bond conjugation operated by the metal coordination, which makes the reductions more difficult. This is confirmed by the examination of the redox potentials of the first one-electron reduction of the series $C_{60}[Mo(CO)_2(phen)(dbm)]_n$, $C_{60}[Pt(PEt_3)_2]_n$, and $C_{60}[S_2Fe_2(CO)_6]_n$ with respect to that of free C_{60} reported in Table 2: in spite of the fact that all complexes are η^2-6:6 coordinated, either negative or positive redox shifts occur.

Table 2. Potential shifts (in V) for the first one-electron reduction of the complexes $(C_{60})[MoL]_n$ [L = $(CO)_2(phen)(dbm)$], $C_{60}[Pt(PEt_3)_2]_n$, and $C_{60}[S_2Fe_2(CO)_6]_n$ with respect to the $[C_{60}]^{0/-}$ couple

Complex	$\Delta E^{\circ\prime}_{0/-}$	Solvent	Reference
$(C_{60})[MoL]$	−0.14	CH_2Cl_2	[a]
$(C_{60})[MoL]_2$	−0.28	CH_2Cl_2	[a]
$(C_{60})[MoL]_3$	−0.41	CH_2Cl_2	[a]
$(C_{60})[Pt(PEt_3)_2]$	−0.34	THF	6
$(C_{60})[Pt(PEt_3)_2]_2$	−0.65	THF	6
$(C_{60})[Pt(PEt_3)_2]_3$	−1.07	THF	6
$(C_{60})[Pt(PEt_3)_2]_4$	−1.45	THF	6
$(C_{60})[(S_2)Fe_2(CO)_6]$	+0.02	1,2-$Cl_2C_6H_4$	2
$(C_{60})[(S_2)Fe_2(CO)_6]_2$	+0.02	1,2-$Cl_2C_6H_4$	2
$(C_{60})[(S_2)Fe_2(CO)_6]_3$	+0.06	1,2-$Cl_2C_6H_4$	2

[a] Present work.

The X-band EPR spectrum of the monoanions $[(\eta^2\text{-}C_{60})M(CO)_2(phen)(dbm)]^-$ (M = Mo, W) electrogenerated in dichloromethane solutions have been previously discussed.[7b] As a matter of fact, the freshly electrogenerated monoanion $[(\eta^2\text{-}C_{60})Mo(CO)_2(phen)(dbm)]^-$ exhibits a well separated, broad, and unresolved axial structure having $g_{\parallel} > g\perp \neq g_{electron} = 2.0023$, Figure 4a.

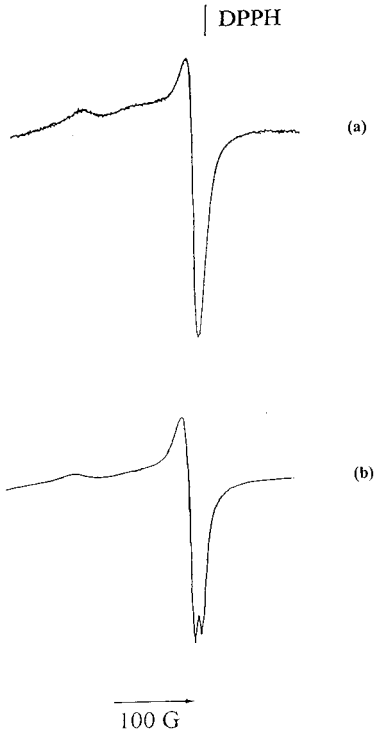

Figure 4. X-band EPR spectra of $[(\eta^2\text{-}C_{60})\{Mo(CO)_2(phen)(dbm)\}]^-$ in CH_2Cl_2 recorded at 100 K: (a) just after its electrogeneration at 250 K; (b) after exposure to air for a few seconds

Even if the low abundance of the Mo-95/97 nuclei does not allow their satellite hyperfine resolution to be detected ($I_{Mo\text{-}95}$ = 5/2; natural abundance = 15.7%; $I_{Mo\text{-}97}$ = 5/2; natural abundance = 19.5%), the width of the signal coupled to its g_i values could be interpreted as being due to a paramagnetic species possessing a partial metallic character, i.e., the fullerene based SOMO of the monoanion could have a significant contribution from the 4d-Mo AO's. In spite of the stability of the monoanion under inert atmosphere, handling the sample even for short times in air causes the appearance of a new absorption that is quite coincident with that of free $[C_{60}]^-$, Figure 4b.

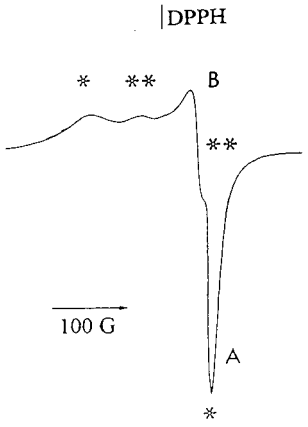

Figure 5. X-band EPR spectrum of a CH_2Cl_2 solution of the freshly electrogenerated monoanion $[(C_{60})\{Mo(CO)_2(phen)(dbm)\}_2]^-$ recorded at 100 K

Figure 5 shows the low-temperature EPR spectrum of the freshly electrogenerated monoanion $[C_{60}\{Mo(CO)_2(phen)(dbm)\}_2]^-$, and exhibits two partially overlapping signals [hereafter indicated as A (*) and B (**), respectively], both of them being resolved in axial structures with $g_{\|i} > g_{\perp i} \neq g_{electron} = 2.0023$.

Table 3. X-band EPR parameters of the electrogenerated monoanions $[(C_{60})\{MoL\}_n]^-$, [L = $(CO)_2$(phen)(dbm)] recorded at 100 K in CH_2Cl_2 solution. ($g_i = \pm 0.002$)

Monoanion	$g_{\|}$ [a]	$g_{\perp}$ [a]	$<g>$ [a][b]	g_{iso}
$[(C_{60})\{MoL\}]^-$	2.089	2.014	2.039	–
$[(C_{60})\{MoL\}_2]^-$ (A)*	2.058	1.960	1.993	–
$[(C_{60})\{MoL\}_2]^-$ (B)**	2.016	1.973	1.987	–
$[C_{60}]^-$	–	–	1.998	1.995[c]

[a] T = 100 K. – [b] $<g> = (g_{\|} + 2g_{\perp})/3$. – [c] T = 295 K; * = outer signals, ** inner signals.

The relevant best fit parameters are collected in Table 3 and can be suitably computed, taking into account an S = 1/2 Electron Spin Hamiltonian for the two axial signals. The line-shape analysis reveals that the species A and B are present in a 2:1 molar ratio. It does not seem too ventured to assume that the two paramagnetic species are geometrical isomers, with the major component likely possessing the commonest geometry in which the two Mo fragments lie at the opposite sides of C_{60}.[8,11] Also, no EPR evidence for the Mo-95/97 satellite hyperfine resolution has been gained in this case, but the spectral pattern might be interpreted in the sense that the overall SOMO likely has a contribution from either the fullerene 2p-C AO's or the two 4d-Mo AO's.

As in the case of the monoadduct, raising the temperature at the glassy-fluid transition induces disappearance of the anisotropic features, while the typical sharp signal of free $[C_{60}]^-$ anion appears as a minor species. A fast refreezing of the solution does not, however, restore the original signal, as is the case for $[(C_{60})Mo(CO)_2(phen)(dbm)]^-$,[7b] thus pointing out that $[(C_{60})\{Mo(CO)_2(phen)(dbm)\}_2]^-$ is more reactive with traces of air than $[(C_{60})Mo(CO)_2(phen)(dbm)]^-$.

Because of the multiple species present in a solution of $(C_{60})[Mo(CO)_2(phen)(dbm)]_3$, we did not attempt the EPR characterization of its monoanion.

Electrochemistry of $(\eta^2\text{-}C_{70})[Mo(CO)_2(phen)(dbm)]$

Figure 6 and Figure 7 show the cyclic voltammetric behaviour of $(C_{70})[Mo(CO)_2(phen)(dbm)]$, in comparison with that of free C_{70}, at different potential windows.

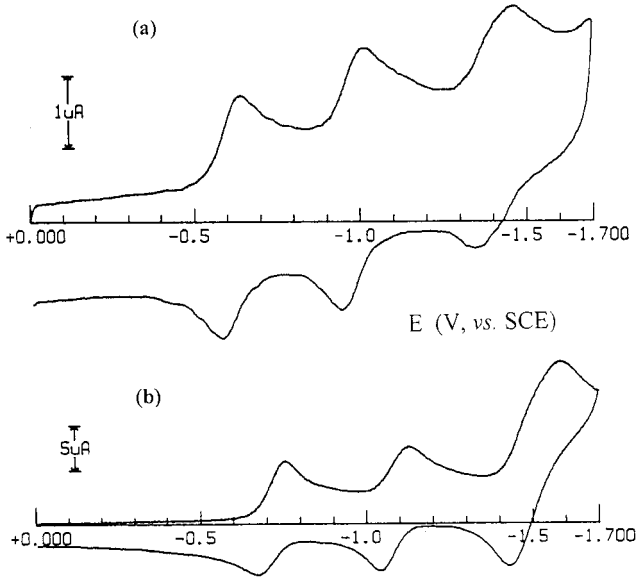

Figure 6. Cyclic voltammetric responses recorded at a platinum electrode in CH_2Cl_2 solutions containing $[NBu_4][PF_6]$ (0.2 mol dm^{-3}) and: (a) C_{70} (saturated solution); (b) $C_{70}[Mo(CO)_2(phen)(dbm)]$ ($4\cdot10^{-4}$ mol dm^{-3}); scan rate 0.2 Vs^{-1}, T = −10 °C

It is easily seen from the first three cathodic waves, Figure 6, that the presence of the Mo fragment also induces a cathodic shift of the first two C_{70}-centred one-electron reductions with respect to free C_{70}. Nevertheless, at variance with the C_{60} analog, the third cathodic process appears as an essentially overlapping two-electron step. Based on the reversibility of such processes and on the fact that the one-electron reductions of either the molybdenum fragment in $(C_{60})[Mo(CO)_2(phen)(dbm)]$ or that of the precursor $Mo(CO)_2(phen)(dbm)_2$ occur at more negative potential values (−1.9 V and −1.7 V, respectively),[7b] we are keen to assume that this closely-spaced two-electron step is due to the substantial concomitance of the third and fourth one-electron reductions of the C_{70} moiety. Finally, as far as the fourth reduction process is concerned, Figure 7, the appear-

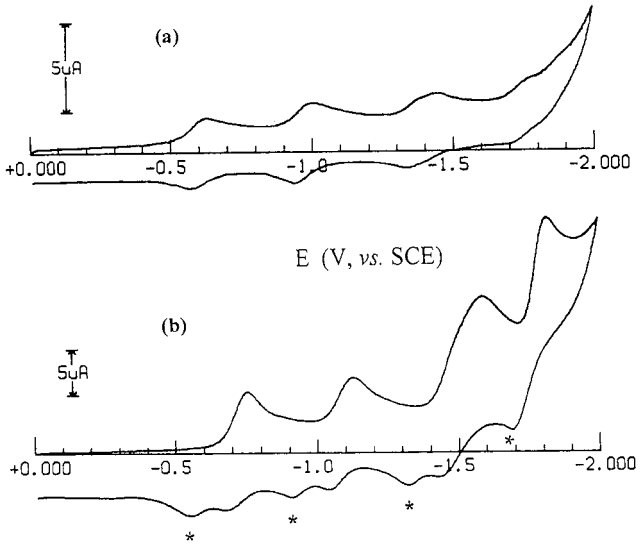

Figure 7. Cyclic voltammetric responses recorded under the same experimental conditions as for Figure 5, along a more extended potential window

ance in the back-scan of the sequential re-oxidations of the free fulleride anions (starred peaks) points out that it induces C_{70} decomplexation as a consequence of the simple EC step:

$$[M^0(\eta^2\text{-}C_{70})]^{4-} \xrightarrow{+e^-} [M^{-1}(\eta^2\text{-}C_{70})]^{5-} \xrightarrow{k} [M]^- + [C_{70}]^{4-}$$

$M = Mo(CO)_2(phen)(dbm)$

In summary, the reduction pathway of $(C_{70})[Mo(CO)_2(phen)(dbm)]$ is rather different from that of its C_{60} analogue in two respects: (i) the electronic perturbation played by the metal fragment forces the third and fourth one-electron additions to C_{70} to become concomitant; (ii) the fourth reduction involves a simple metal-centred process, whereas in the C_{60} derivative it involves the following metal-centred ECE mechanism:

$$[M^0(\eta^2\text{-}C_{60})]^{3-} \xrightarrow{+e^-} [M^{-1}(\eta^2\text{-}C_{60})]^{4-} \xrightarrow{k} [M]^- + [C_{60}]^{3-}$$

$$[C_{60}]^{3-} \xrightarrow{+e^-} [C_{60}]^{4-}$$

$M = Mo(CO)_2(phen)(dbm)$

The relevant electrochemical data are compiled in Table 1.

Finally, it is interesting to note that under the same experimental conditions, the cathodic shift induced by appending the $Mo(CO)_2(phen)(dbm)$ unit to C_{70} is lower than for C_{60}, (0.10 V vs. 0.15 V), thus suggesting that the extent to which the double bond conjugation is broken by the coordination to C_{70} should be lower than with C_{60}. Unfortunately, such a conclusion cannot be generalised because in the case of $(C_{70})[(S_2)Fe_2(CO)_6]$ and $(C_{60})[(S_2)Fe_2(CO)_6]$ the shifts with respect to the corresponding free fullerenes are −0.01 V and +0.02 V, respectively,[2] indicating that the extent of double bond saturation is higher in the C_{70} complex. Underlined that in the last case the interaction of the metal centre with the fullerene ligand is mediated by the disulfur bridge, more data on complexes bearing the same metal fragment directly bound to both C_{60} and C_{70} are needed to clarify such an electronic aspect.

Experimental Section

Material and apparatus for electrochemistry and coupled ESR measurements have been previously described.[7b] All the potential values are referred to the saturated calomel electrode (SCE). Under the present experimental conditions, the one-electron oxidation of ferrocene occurs at $E^{\circ\prime} = +0.34$ V in the temperature range from −10 °C to +10 °C, and at $E^{\circ\prime} = +0.35$ V at +20 °C. The external magnetic field H_0 for ESR spectroscopy was calibrated by using a DPPH powder sample ($g_{DPPH} = 2.0036$). Computer simulation of the ESR spectra was carried out by using the SIM14 A program.[19]

Synthesis: All the reactions were carried out under a nitrogen atmosphere with the use of standard Schlenk techniques. The preparation of $(\eta^2\text{-}C_{60})[Mo(CO)_2(o\text{-phen})(dbm)]$ has been previously reported.[7a]

$(C_{60})[Mo(CO)_2(o\text{-phen})(dbm)]_n$ (n = 2, 3): $Mo(CO)_2(o\text{-phen})(dbm)_2$ (178 mg, 0.225 mmol) was added to a solution of C_{60} (54 mg, 0.075 mmol) in benzene (25 cm^3). The mixture was heated under reflux for 2 h, and then concentrated. The resulting dark green solution was separated by column chromatography (silica gel) using benzene/THF (7:1, then 5:1, and finally 4:1) as eluent. The two main chromatography bands were collected separately, and the solvents were removed. Both the residues were washed with petroleum ether (ca. 30−60 °C) and pentane, and then dried in vacuo to give dark green powders. One is $(C_{60})[Mo(CO)_2(o\text{-phen})(dbm)]_2$ (60 mg, 44%). − Found: C 73.70, H 2.84, N 3.53; calcd.: C 73.04, H 3.07, N 3.04. − IR: $\tilde{\nu}_{max}$ = 1963 (s), 1898 (s) [νC≡O], 1689 (s) [νC=O], 1423 (m), 1159 (s), 573 (w), 525 (m) [νC_{60}]; 428(w) [ν(Mo-(η^2-C=C))], 367cm^{-1} (w) [ν(Mo−N)]. − UV/Vis (CH_2Cl_2): λ_{max} = 258 nm. − The other is $(C_{60})[Mo(CO)_2(o\text{-phen})(dbm)]_3$ (30 mg, 17%). − Found: C 71.34, H 3.05, N 3.24; calcd.: C 69.00, H 3.53, N 3.50. − IR: $\tilde{\nu}_{max}$ [cm^{-1}] = 1959 (s), 1894 (s) [νC≡O]; 1690 (s) [νC=O]; 1422 (m), 1157 (s), 570 (w), 522 (m) [νC_{60}]; 430 (w) [ν(Mo-{η^2-C=C})]; 371(w) [ν(Mo−N)]. − UV/Vis (CH_2Cl_2): λ_{max} [nm]: 258.

$(\eta^2\text{-}C_{70})[Mo(CO)_2(o\text{-phen})(dbm)]$: $Mo(CO)_2(o\text{-phen})(dbm)_2$ (39 mg, 0.05 mmol) was added to a solution of C_{70} (42 mg, 0.05 mmol) in benzene (25 cm^3). The mixture was heated under reflux for 1 h, and then concentrated. The resulting red-brown solution was separated by column chromatography (silica gel) using benzene/acetone (12:1) as eluent. The main chromatography band was collected. The solvents were removed and the residue dried in vacuo to give a red brown powder, (23 mg, 32%). Crystals were obtained by slow diffusion of pentane into a dichloromethane solution. − Found: C 81.90, H 2.55, N 1.85; calcd. for $C_{70}[Mo(CO)_2(o\text{-phen})(dbm)]$: C 82.29,; H 2.01, N 2.00}. IR: $\tilde{\nu}_{max}$ [cm^{-1}] = 1957 (s), 1890 (s) [νC≡O]; 1684(s) [ν(C=O)]; 1427 (s), 1410 (s), 1159 (s), 1131 (m), 797 (w), 674 (w), 640 (w), 573 (w), 535 (w), 456 (w) [νC_{70}]; 434 (w) [ν(Mo-{η^2-C=C})]; 367 (w) [ν(Mo−N)]. − UV/Vis (CH_2Cl_2): λmax [nm]: 238. − ^{1}H NMR: δ_H (Solvent $CDCl_3$ + CS_2, standard $SiMe_4$): 0.9 (t, 6 H, $CH_2CH_2CH_2CH_3$), 1.3 (m, 4 H, $CH_2CH_2CH_2CH_3$), 1.5 (m, 4 H, $CH_2CH_2CH_2CH_3$), 4.1 (t t, 4 H, $O{=}C{-}OCH_2CH_2CH_2CH_3$, s, 2 H, =CH), 7.8 (m,m, 2 H, $H^{3,8}$ of

phen), 7.9 (d, 2 H, $H^{5,6}$ of phen), 8.4 (m, 2 H, $H^{4,7}$ of phen), 9.0 (d,d, 2 H, $H^{2,9}$ of phen). – ^{13}C NMR: δ_C (Solvent $CDCl_3$ + CS_2): 14 (s, $CH_2CH_2CH_2CH_3$), 20 (s, $CH_2CH_2CH_2CH_3$), 31 (s, $CH_2CH_2CH_2CH_3$), 64 (s, $O{=}C{-}OCH_2CH_2CH_2CH_3$), 77 (dd, *C*=*C* of C_{70} and dbm), 124–163 (s, 41 signals comprising 6 phen and 35 C_{70} signals, 1 signal omitted), 172 (s, *C*=O)

Acknowledgments

P. Z. and his research group gratefully acknowledge the financial support of the University of Siena (ex quota 60%). K. T. and co-workers acknowledge the financial support by National Natural Science Foundation of China (Project No. 298730001).

[1] [1a]Q. Xie, E. Pérez-Cordero, L. Echegoyen, *J. Am. Chem. Soc.* **1992**, *114*, 3978. – [1b]Q. Li, F. Wudl, C. Thilgen, R. L. Whetten, F. Diederich, *J. Am. Chem. Soc.* **1992**, *114*, 3994. – [1c]C. Boudon, J.-P. Gisselbrecht, M. Gross, A. Hermann, M. Rüttimann, J. Crassous, F. Cardullo, L. Echegoyen, F. Diederich, *J. Am. Chem. Soc.* **1998**, *120*, 7860.

[2] M. D. Westmeyer, T. B. Rauchfuss, A. K. Verma, *Inorg. Chem.* **1996**, *35*, 7140.

[3] A. N. Chernega, M. L. H. Green, J. Haggitt, A. H. H. Stephens, *J. Chem. Soc., Dalton Trans.* **1998**, 755.

[4] [4a]J. T. Park, H. Song, J.-J. Cho, M.-K. Chung, J.-H. Lee, I.-H. Suh, *Organometallics* **1998**, *17*, 227. – [4b]H. Song, K. Lee, J. T. Park, M.-G. Choi, *Organometallics* **1998**, *17*, 4477.

[5] J. T. Park, J.-J. Cho, H. Song, C.-S. Jun, Y. Son, J. Kwak, *Inorg. Chem.* **1997**, *36*, 2698.

[6] S. A. Lerke, B. A. Parkinson, D. H. Evans, P. J. Fagan, *J. Am. Chem. Soc.* **1992**, *114*, 7807.

[7] [7a]K. Tang, S. Zheng, X. Jin, H. Zeng, Z. Gu, X. Zhou, Y. Tang, *J. Chem. Soc., Dalton Trans.* **1997**, 3585. – [7b]P. Zanello, F. Laschi, M. Fontani, C. Mealli, A. Ienco, K. Tang, X. Jin, L. Li, *J. Chem. Soc., Dalton Trans.* **1999**, 965.

[8] [8a]A. L. Balch, J. W. Lee, B. C. Noll, M. M. Olmstead, *J. Am. Chem. Soc.* **1992**, *114*, 10984. – [8b]A. L. Balch, J. W. Lee, B. C. Noll, M. M. Olmstead, *Inorg. Chem.* **1994**, *33*, 5238.

[9] M. Rasinkangas, T. T. Pakkanen, T. A. Pakkanen, M. Ahlgrén, J. Rouvinen, *J. Am. Chem. Soc.* **1993**, *115*, 4901.

[10] I. J. Mavunkal, Y. Chi, S.-M. Peng, G.-H. Lee, *Organometallics* **1995**, *14*, 4454.

[11] T. Kusukawa, W. Ando, *J. Organomet. Chem.* **1998**, *561*, 109 .

[12] A. L. Balch, J. W. Lee, M. M. Olmstead, *Angew. Chem. Int. Ed. Engl.* **1992**, *31*, 1356.

[13] H.-F. Hsu, J. R. Shapley, *J. Am. Chem. Soc.* **1996**, *118*, 9192.

[14] H.-F. Hsu, S. R. Wilson, J. R. Shapley, *Chem. Commun.* **1997**, 1125.

[15] M. Soimasuo, T. T. Pakkanen, M. Ahlgrén, T. A. Pakkanen, *Polyhedron* **1998**, *17*, 2073.

[16] A. L. Balch, L. Hao, M. M. Olmstead, *Angew. Chem. Int. Ed. Engl.* **1996**, *35*, 188.

[17] [17a] K. Lee, H.-F. Hsu, J. R. Shapley, *Organometallics* **1997**, *16*, 3876. – [17b] K. Lee, J. R. Shapley, *Organometallics* **1998**, *17*, 3020.

[18] P. J. Fagan, J. C. Calabrese, B. Malone, *J. Am. Chem. Soc.* **1991**, *113*, 9408.

[19] J. P. Lozos, B. M. Hoffman, C. G. Franz, *QCPE* **1973**, *243*, 11.

Received November 10, 1999
[I99399]